Pediatric Radiology (2020) 50:1669–1679
https://doi.org/10.1007/s00247-020-04841-8

MINISYMPOSIUM: IMAGING OF SKELETAL DYSPLASIA

Neuroimaging and calvarial findings in achondroplasia

Fatma Ceren Sarioglu[1] · Orkun Sarioglu[2] · Handan Guleryuz[1]

Received: 21 April 2020 / Revised: 7 July 2020 / Accepted: 7 September 2020 /

Abstract
Achondroplasia is the most common hereditary form of dwarfism and is characterized by short stature, macrocephaly and various skeletal abnormalities. The phenotypic changes are mainly related to the inhibition of endochondral bone growth. Besides the several commonly known physical features that are characteristic of this syndrome, achondroplasia can affect the central nervous system. The impact on the central nervous system can cause some important clinical conditions. Thus, awareness of detailed neuroimaging features is helpful for the follow-up and management of complications. Although the neuroimaging findings in children with achondroplasia have been noted recently, no literature has specifically reviewed these findings extensively. Radiologists should be familiar of these findings because they have an important role in the diagnosis of achondroplasia and the recognition of complications. The aim of this pictorial essay is to review and systematize the distinctive characteristics and abnormalities of the central nervous system and the calvarium in children with achondroplasia.

Keywords Achondroplasia · Brain · Children · Computed tomography · Magnetic resonance imaging · Skull base

Introduction

Achondroplasia, which is the most common skeletal dysplasia, is characterized by disproportionately short stature with rhizomelic shortening of the extremities. Specific mutations of the fibroblast growth factor receptor 3 (*FGFR3*) gene cause defective endochondral bone growth [1]. Various mutations in the *FGFR3* gene are also responsible for a number of disorders such as hypochondroplasia, thanatophoric dysplasia, Crouzon syndrome and Muenke syndrome [2]. The phenotypic changes are mainly related to the inhibition of endochondral bone growth.

Achondroplasia can lead to various neurologic and otorhinolaryngologic risks and symptoms including motor delays, hydrocephalus, obstructive apnea, otitis media, sinusitis, dental malocclusion and cervical myelopathy [2–5].

Many neuroimaging findings as well as skull base abnormalities are associated with achondroplasia. Although many articles describe brain findings of hypochondroplasia and thanatophoric dysplasia, the neuroimaging findings in children with achondroplasia have only recently drawn more attention [6–8]. The neuroimaging findings in achondroplasia and its complications or symptoms are summarized in Table 1. To understand the implications of brain and calvarial involvement of achondroplasia, familiarity with the anatomical changes is essential. In this pictorial essay, we review several imaging features in children with achondroplasia that should be carefully evaluated in neuroimaging studies.

Skull

Macrocephaly with prominent forehead, midface hypoplasia and skull asymmetry

Macrocephaly, which is defined as a head circumference more than two standard deviations above the mean value for a given age and gender, is a common phenotypic feature of achondroplasia (Fig. 1). Frontal and parietal bossing is demonstrated in children with achondroplasia who have macrocephaly. Ventriculomegaly and enlarged subarachnoid spaces are often associated with the delay in closure of the sutures and macrocephaly [2, 9].

✉ Fatma Ceren Sarioglu
drcerenunal@gmail.com

[1] Department of Radiology, Division of Pediatric Radiology, Dokuz Eylul University School of Medicine, 35340 Balcova, Izmir, Turkey

[2] Department of Radiology, Tepecik Training and Research Hospital, Health Sciences University, Izmir, Turkey

Table 1 The neuroimaging findings and associated clinical conditions in achondroplasia

	Imaging feature	Associated clinical condition
Calvarium	Macrocephaly with prominent forehead	Hydrocephalus
	Midface hypoplasia	Dental malocclusion, speech difficulties
	Skull asymmetry	Craniosynostosis
	Short clivus and narrowing of the skull base	Hydrocephalus, increased intracranial pressure
	Foreshortening of the carotid canals	
	Temporal bone changes	Otitis media, hearing loss, apnea
	Poor development of mastoid air cells	
	Towering of petrous ridge	
	Vertically orientated geniculate ganglion	
	Downward oval window	
	Horizontally orientated scutum	
	Ossicular anomalies	
Brain	Ventriculomegaly	Macrocephaly, increased intracranial pressure
	Enlarged subarachnoid spaces	Macrocephaly, increased intracranial pressure
	Enlarged suprasellar cistern ± empty sella	Pituitary-related endocrine dysfunction
	Decreased optic nerve-base angle	
	Vertically orientated straight sinus	
	Increased tentorial angle	
	Prominent emissary veins and meningeal vessels	
	Temporal lobe anomalies	Seizures, cognitive deficits
	Deep transverse sulcus or sagittal cleft	
	Incomplete hippocampal inversion	
	Oversulcation of mesial temporal lobe and calcar avis	
	Abnormal triangular shape of the temporal horn of lateral ventricle	
	Loss of differentiation of gray white matter	
	Megalencephaly and temporal lobe enlargement	
Craniocervical junction	Narrowing of foramen magnum	Neurologic, respiratory, cardiopulmonary symptoms
	Myelopathy	

Midface hypoplasia occurs as a result of impaired endochondral bone formation and is characterized by depressed nasal bridge, maxillary hypoplasia and prominent forehead. Mandibular growth is spared because intramembranous ossification is the predominant development mechanism of the mandible [2, 3]. Hypoplastic midface can cause several clinical symptoms such as dental malocclusion, speech difficulties and upper respiratory tract obstruction [3]. Three-dimensional images are useful to demonstrate this finding (Fig. 2).

Skull asymmetry, which might be related to craniosynostosis, is better demonstrated on axial or coronal sections (Fig. 3). Crouzon syndrome and thanatophoric dysplasia, which are some of the *FGFR3* gene mutations, are the well-known disorders associated with craniosynostosis. However, it is not uncommon in achondroplasia [2]. Motor retardation is reported in children with achondroplasia who have skull asymmetry [9].

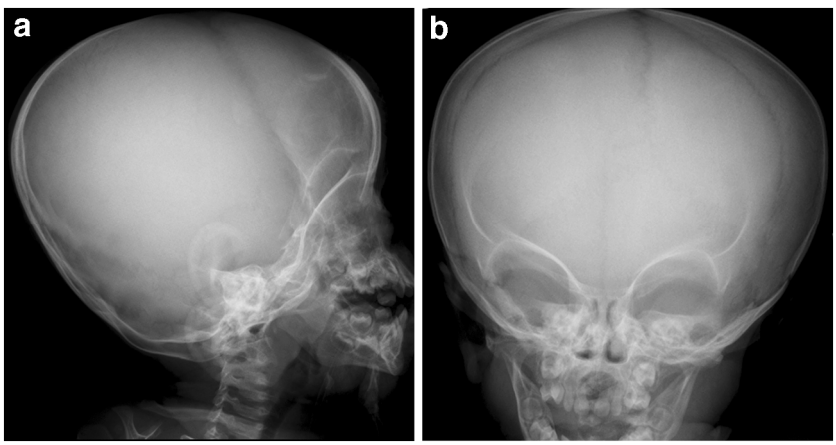

Fig. 1 Macrocephaly and prominent forehead in a 7-year-old girl with achondroplasia. **a, b** Lateral (**a**) and anteroposterior (**b**) skull radiographs show macrocephaly with frontal and parietal bossing

Short clivus and narrowing of the skull base and foreshortening of the carotid canals

Short clivus and narrowing of the skull base are crucial findings that require special attention while evaluating the intracranial structures (Fig. 4). Narrowing of the skull base alters the cerebrospinal fluid dynamics and induces venous outflow obstruction because of reduction in the jugular foramen diameter. This mechanism leads to increased intracranial venous pressure, ventriculomegaly and macrocephaly [10].

The carotid canal normally lies forward and medially in the petrous part of the temporal bone till it reaches the lateral side of the clivus. The normal size of the carotid canals varies depending on age, gender, ethnicity and genetic factors. The foreshortened carotid canals manifest as a result of hypoplastic skull base in children with achondroplasia. Additionally, the distal ends of the carotid canals tend to locate more closely to each other in the midline [11] (Fig. 4). Cobb et al. [11] reported that the average distance between the distal ends of the internal acoustic canals in achondroplasia was 48.0 mm, whereas it was 67.0 mm in non-achondroplastic patients. There has not been any report on whether this finding is associated with the carotid artery stenosis.

Temporal bone anomalies

Squamous and tympanic parts of the temporal bone develop by intramembranous ossification, whereas petrous and mastoid parts ossify endochondrally [12]. Middle ear ossicles also undergo endochondral ossification [11]. The temporal bone findings in achondroplasia are associated with endochondral ossification defects. The otolaryngologic complications include apnea, because of upper airway obstruction, and otitis media, which might be accompanied by hearing loss and delayed speech [4].

- **Poor development of mastoid air cells:** Mastoid air cells are not well-pneumatized without mastoid sclerosis in achondroplasia [11] (Fig. 5).

Fig. 3 Skull asymmetry in an 8-year-old boy with achondroplasia. Axial CT demonstrates subtle asymmetrical bulging of the right frontal bone. The child does not have craniosynostosis

- **Towering of petrous ridge:** The upward tilted position of the medial part of the petrous bone, when compared to the lateral part, causes a characteristic "tower-like appearance" on coronal slices [11] (Fig. 6). Internal acoustic canals also locate more vertically because of the upward tilting of the petrous bone.
- **Vertically orientated geniculate ganglion:** The labyrinthine segment of the facial nerve courses anterolaterally from the internal auditory canal and superior to the cochlea until it reaches the geniculate ganglion. At the geniculate ganglion, the facial nerve turns posteriorly to become the tympanic segment. The normal position of the geniculate ganglion is horizontal to the petrous bone. The angle between the tympanic and the labyrinthine segment

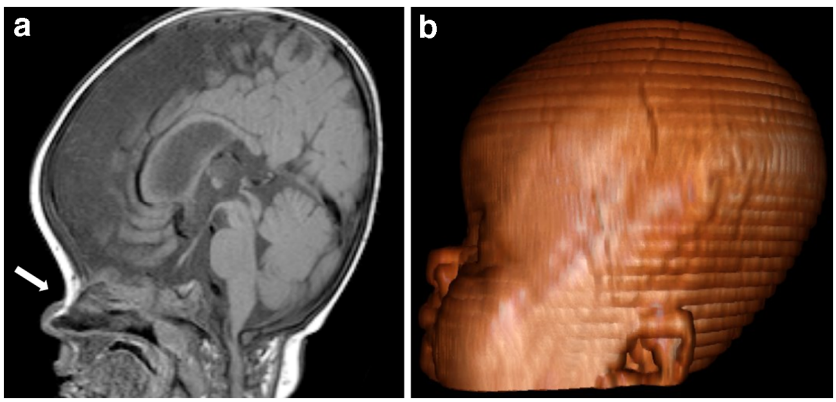

Fig. 2 Midface hypoplasia and depressed nasal bridge in a 6-year-old girl with achondroplasia. **a, b** Sagittal (**a**) and three-dimensional reconstructed (**b**) T1-weighted MR images (repetition time/echo time: 500/15 ms) show the depressed nasal bridge (*arrow*) with prominent forehead and hypoplastic midface

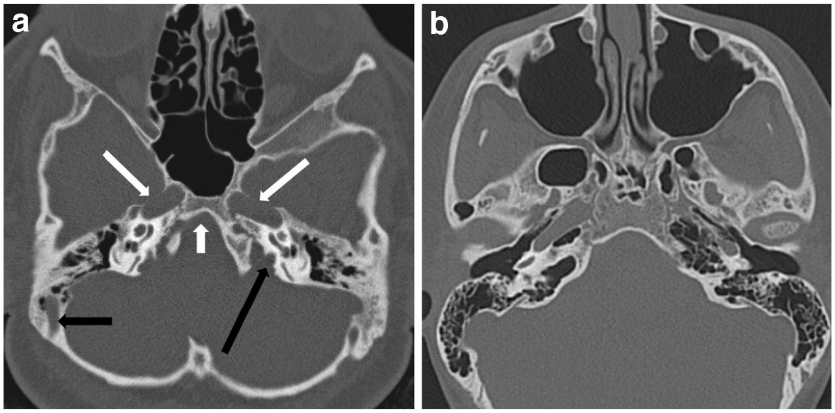

Fig. 4 Short clivus and narrowing of the skull base and foreshortening of carotid canals in a 14-year-old boy with achondroplasia. **a** Axial CT image shows the short clivus with narrowing of the skull base (*short white arrow*) and foreshortened carotid canals (*long white arrows*). Note the narrowing of the jugular foramen (*long black arrow*) and enlarged mastoid emissary vein (*short black arrow*). The distal ends of the carotid canals are located more closely to each other. **b** Axial CT image of a gender- and age-matched normal child for comparison shows the normal appearance of the skull base

of the facial nerve is obtuse. In children with achondroplasia, it locates vertically because of the more vertical orientation of the internal acoustic canals and the angle narrows (Fig. 7). A rotation of the cochlea might also be associated [11].

- **Downward oval window:** The oval window opens to the vestibule of the inner ear. The vestibule is rotated because of the abnormal position of the petrous apex and so the oval window faces downward [11] (Fig. 8).
- **Horizontally orientated scutum:** The appearance of the normal scutum is a vertical bony spur that extends inferiorly from the superior wall of the external auditory canal. In achondroplasia, the external acoustic canals rotate as well as the internal acoustic canals. As a result, the scutum locates horizontally [11] (Fig. 8).
- **Ossicular anomalies:** There have been no reports that the ossicles change in size or shape in children with achondroplasia. However, rotation can also affect the ossicles, especially the body of the malleus and the long process of the incus. It causes a "broad ice-cream cone" appearance [11] (Fig. 9). Additionally, the mobility of the ossicles can decrease [13]. It might be related to the rotation of the ossicles and recurrent otitis media. The ossicular anomalies can lead to hearing loss.

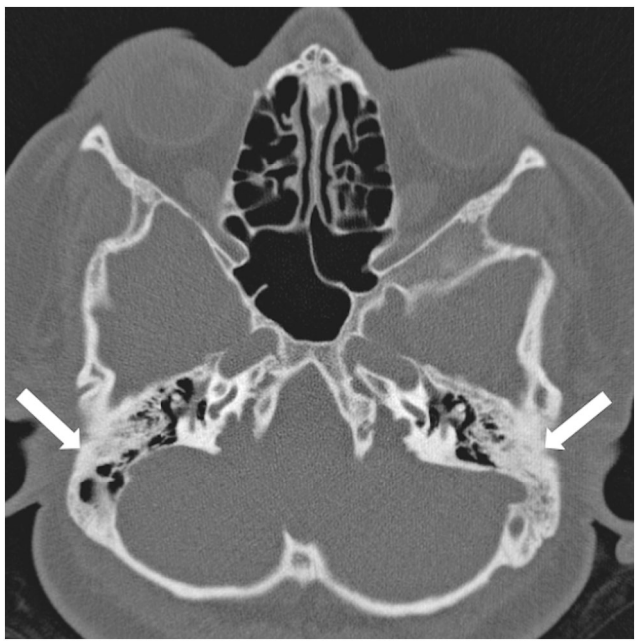

Fig. 5 Poor development of mastoid air cells in the same 14-year-old boy as in Fig. 4. Axial CT image demonstrates the poor mastoid aeration (*arrows*)

Brain

Ventriculomegaly and enlarged subarachnoid spaces

Ventriculomegaly and enlarged subarachnoid spaces are typical brain imaging features of achondroplasia (Fig. 10). A number of studies proposed that the main mechanisms for ventriculomegaly in people with achondroplasia are venous congestion secondary to stenosis at the level of the jugular foramen or thoracic inlet. Foramen magnum stenosis is another cause for ventriculomegaly with obstruction of the basal cisterns, brainstem distortion, and blockage of the fourth-ventricle outlet [10, 14]. Impaired venous drainage at the skull base and chronic dural venous hypertension also lead to the enlargement of subarachnoid spaces [14, 15]. The presence of transependymal cerebrospinal fluid edema should also be observed for decompensated hydrocephalus because it might require ventriculoperitoneal shunt immediately.

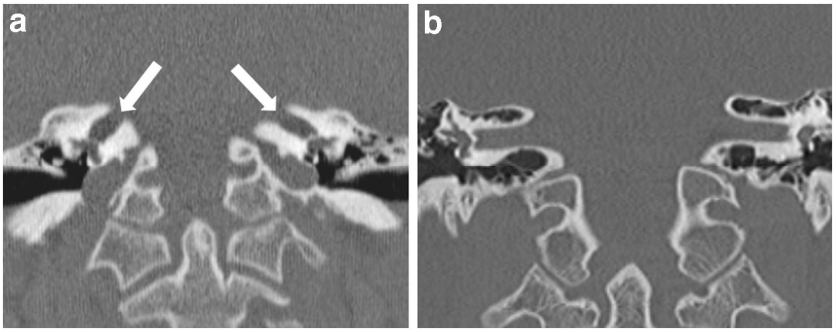

Fig. 6 Petrous ridge towering in a 15-year-old girl with achondroplasia. **a** Coronal CT reconstruction shows the upward tilting of the petrous bone and vertical rotation of internal acoustic canals (*arrows*). **b** Coronal reconstructed CT image of a normal child for comparison shows the normal appearance of the petrous ridge and orientation of the internal acoustic canals

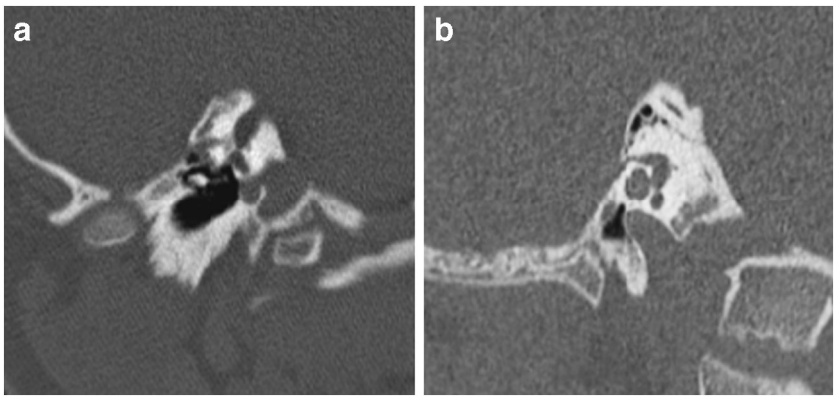

Fig. 7 Vertically orientated geniculate ganglion in the same 15-year-old girl as in Fig. 6. **a** Coronal CT reconstruction of the geniculate ganglion shows the narrow angle with a vertical orientation of the geniculate ganglion. **b** Coronal reconstructed CT image of the geniculate ganglion of a normal child for comparison shows the normal appearance of the geniculate ganglion

Enlarged suprasellar cistern and decreased optic nerve-base angle

An enlarged suprasellar cistern is a result of the same mechanism as enlargement of the subarachnoid spaces (Fig. 11). Empty sella can accompany this finding [9]. Children might present with pituitary-related endocrine dysfunction symptoms.

Optic nerve-base angle also decreases in achondroplasia (Fig. 11). The obtuse angle formed by the intersection of a line between the plane of the cribriform plate and the optic tract is between 140º and 160º in normal people [9]. The angle was reported as varying 115º to 140º in people with achondroplasia [9, 16]. There is no evidence whether this finding causes the visual symptoms.

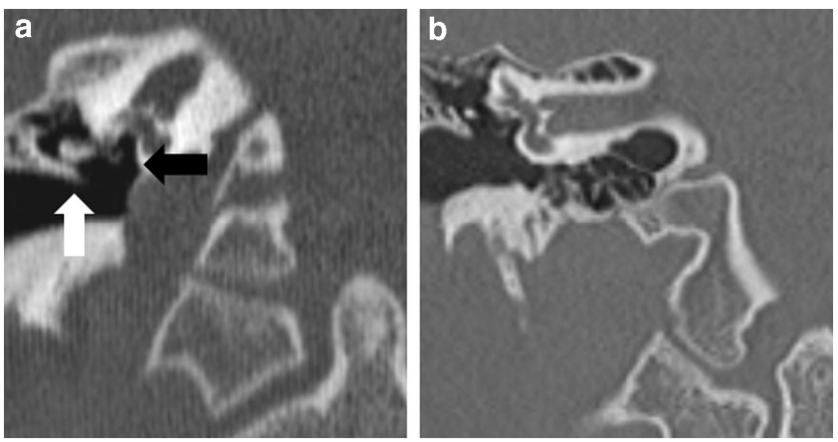

Fig. 8 Downward oval window and horizontally orientated scutum in the same 15-year-old girl as in Fig. 6. **a** Coronal CT reconstruction demonstrates the more vertical position of the oval window (*black arrow*) and the more horizontal position of the scutum (*white arrow*). **b** Coronal reconstruction of CT image in a normal child for comparison shows the normal appearance of the oval window and scutum

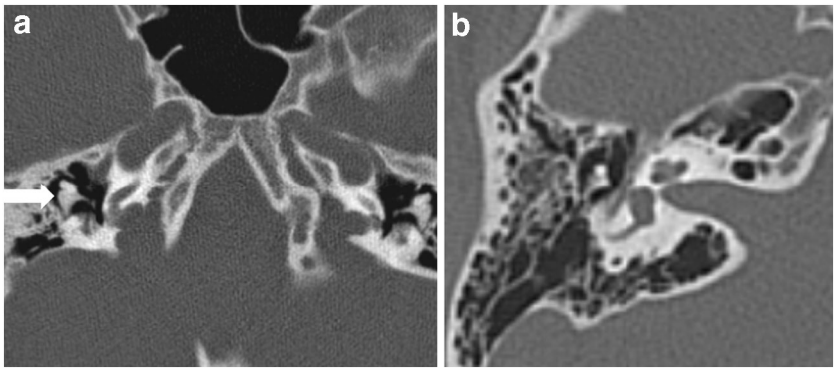

Fig. 9 Broad ice-cream cone sign in the same 15-year-old girl as in Fig. 6. **a** Coronal CT reconstruction demonstrates that the incus appears thicker and shorter, namely as a "broad ice-cream cone" (*arrow*), from the rotation of ossicles. **b** Coronal reconstructed CT image of a normal child for comparison shows a normal ice-cream cone appearance

Vertically orientated straight sinus and increased tentorial angle

Straight sinus and tentorium are more vertical in achondroplasia [9] (Fig. 11). The tentorial angle is measured between a line connecting the nasion with the tuberculum sella and the angle of the straight sinus. Normally, it should measure between 27º and 52º [17]. The angle was found to be between 55º and 70º in people with achondroplasia [9].

Prominent emissary veins and meningeal vessels

The prominent emissary and meningeal vessels are important findings that should be evaluated prior to surgery in children with achondroplasia. T2-weighted gradient echo MR sequence is helpful to recognize this finding (Fig. 12). A number of studies reported that the prominent emissary veins were caused by the narrowing of the foramen magnum and jugular foramen [5, 18]. Conversely, a recent study [8] suggested that there was no significant correlation between the severity of foramen magnum stenosis, stenosis of jugular foramina, and enlargement of emissary veins and meningeal vessels.

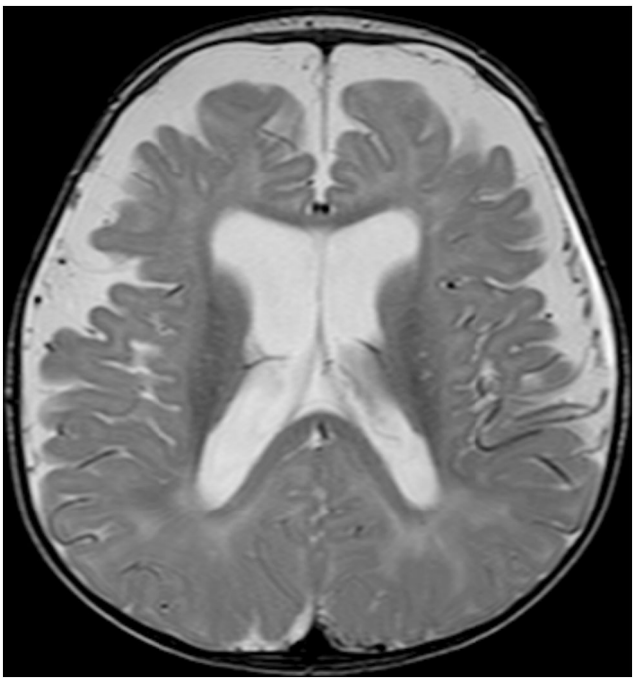

Fig. 10 Ventriculomegaly and enlarged subarachnoid spaces in a 15-month-old boy with achondroplasia. Axial T2-weighted MR image (repetition time/echo time: 5,500/100 ms) shows the ventriculomegaly and prominent subarachnoid spaces in both frontal and parietal regions

Temporal lobe anomalies

Temporal lobe anomalies and accompanying seizures are well-documented findings in other *FGFR3*-related disorders such as hypochondroplasia and thanatophoric dysplasia. They have also been described in people with achondroplasia [6, 19].

- **Deep transverse sulcus or sagittal cleft:** Deep transverse sulcus of the mesial temporal lobe was reported in all children in a study by Manikkam et al. [6], which evaluated the temporal lobe anomalies in 13 children with achondroplasia. Axial MR images are more helpful to demonstrate “deep transverse sulcus,” whereas sagittal images can also be used to recognize this deep sulcus with an alternative definition as “sagittal cleft" (Fig. 13). The finding was also described for other *FGFR3* disorders including hypochondroplasia and thanatophoric dysplasia [20].
- **Incomplete hippocampal inversion:** Incomplete hippocampal inversion was found as the second most prevalent finding in 92% of children with achondroplasia [6]. The *FGFR3* gene has an important role in hippocampal development [21]. In normal hippocampal development, the hippocampal formation inverts within the medial temporal lobe [22]. The appearance of an incomplete hippocampal rotation is characterized by the verticalization of the inferior temporal sulcus on coronal MR images (Fig. 14). It should not be forgotten that the finding can vary individually [22]. Additionally, the size and signal intensity of the hippocampus on MR images can be normal even if the normal hippocampal inversion is absent [23].

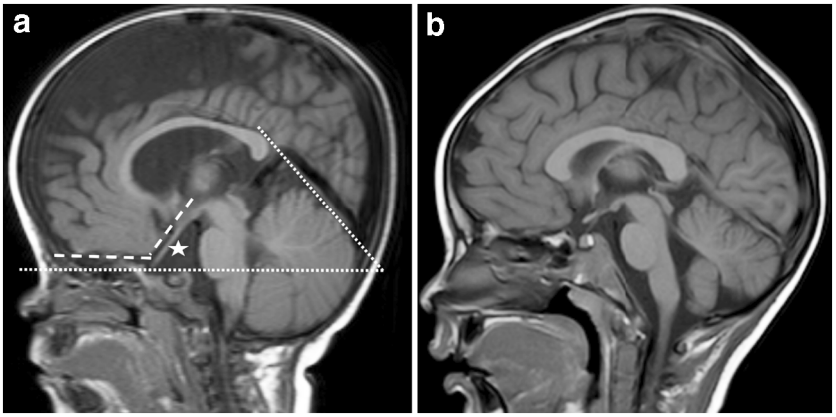

Fig. 11 Enlarged suprasellar cistern, decreased optic nerve-base angle, vertically orientated straight sinus, and increased tentorial angle in a 7-year-old boy with achondroplasia. **a** Sagittal T1-weighted MR image (repetition time/echo time: 500/15 ms) shows the enlarged suprasellar cistern (*star*) with a decreased optic nerve-base angle (*dashed lines*). Straight sinus is more vertical (*dotted lines*). **b** Sagittal T1-weighted MR image of a normal child for comparison shows normal appearances of these findings

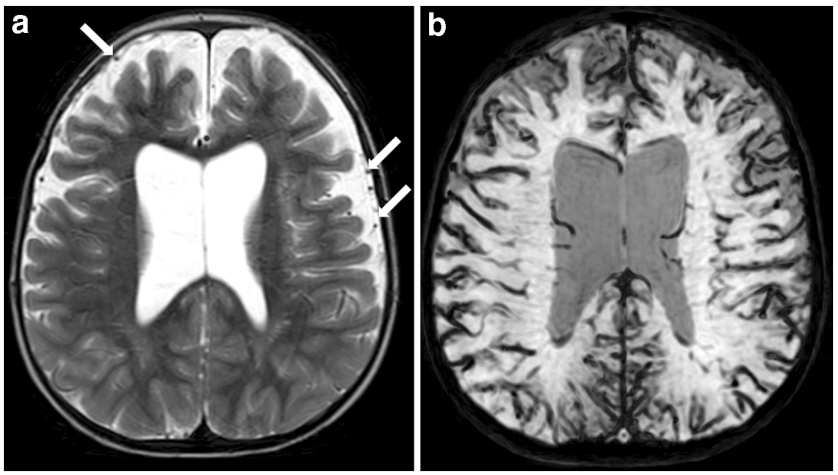

Fig. 12 Prominent meningeal vessels in a 10-year-old boy with achondroplasia. **a** Axial T2-weighted MR image (repetition time/echo time: 5,500/100 ms) shows that the meningeal vessels as slightly enlarged (*arrows*) in enlarged subarachnoid spaces. **b** Susceptibility-weighted MR imaging on axial plane demonstrates the prominent meningeal vessels conspicuously

- **Oversulcation of the mesial temporal lobe and calcar avis:** The oversulcation of the mesial temporal lobe was found as a common finding with a frequency of 85% in children with achondroplasia [6]. Calcar avis, which is produced by the calcarine sulcus, is a term to define the medial wall of the occipital horn of the lateral ventricle. The oversulcation of the mesial temporal lobe can be determined on both coronal and

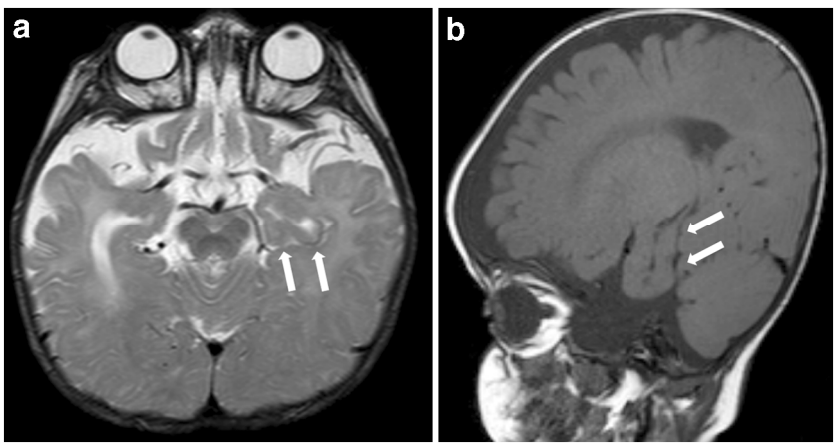

Fig. 13 Deep transverse sulcus and sagittal cleft in the mesial temporal lobe in a 14-month-old boy with achondroplasia. **a** Axial T2-weighted MR image (repetition time/echo time [TR/TE]: 5,500/100 ms) shows a deep transverse sulcus within the left mesial temporal lobe (*arrows*). **b** Sagittal T1-weighted MR image (TR/TE: 500/15 ms) demonstrates the deep transverse sulcus as a cleft (*arrows*)

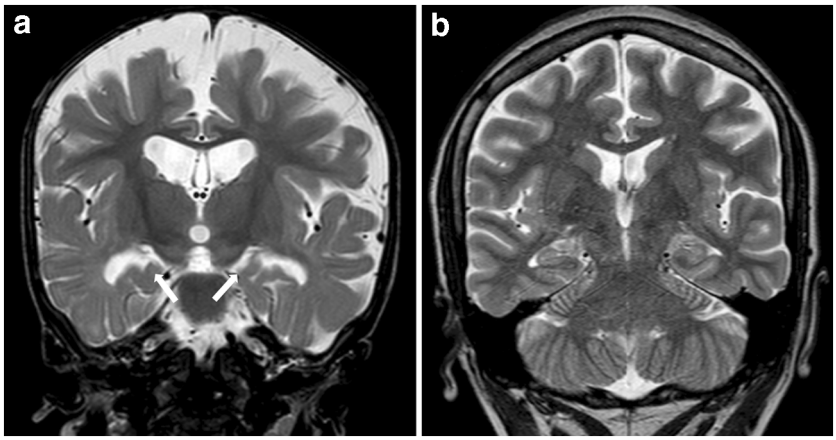

Fig. 14 Incomplete hippocampal inversion in an 8-year-old boy with achondroplasia. **a** Coronal T2-weighted MR image (repetition time/echo time [TR/TE]: 5,500/100 ms) shows bilateral incomplete hippocampal inversion (*arrows*). The finding is more demonstrative on the right side. **b** Coronal T2-weighted MR image (TR/TE: 5,500/100 ms) of a normal child for comparison shows the normal appearance of the hippocampi

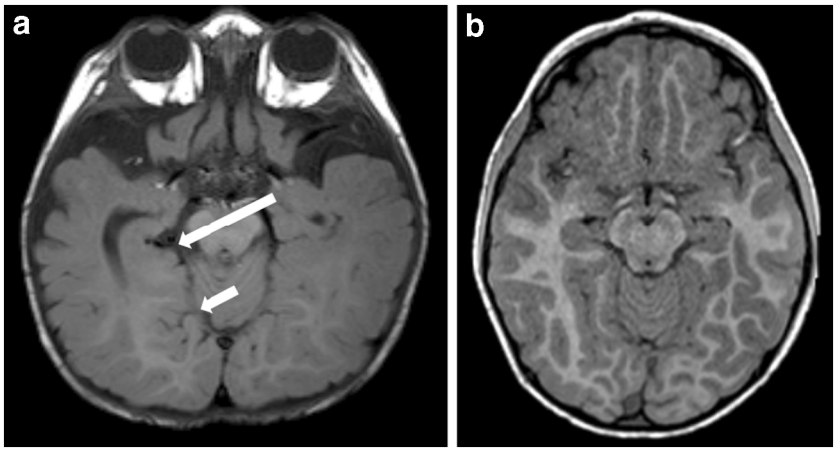

Fig. 15 Oversulcation of mesial temporal lobe and calcar avis in the same 14-month-old boy as in Fig. 13. **a** Axial T1-weighted MR image (repetition time/echo time [TR/TE]: 500/15 ms) shows oversulcation of the mesial temporal lobe (*long arrow*) and extension of the oversulcation to the calcar avis (*short arrow*). **b** Axial T1-weighted MR image (TR/TE: 500/15 ms) of a normal child for comparison shows the normal sulcation pattern of the mesial temporal lobe and calcar avis

axial images. Axial images are also useful in evaluating the extent of oversulcation to the calcar avis (Fig. 15). The frequency of oversulcation of the calcar avis (69%) was found to be less than the oversulcation of mesial temporal lobe [6]. Although abnormal sulcation is also a well-known finding in thanatophoric dysplasia, there are some differences between these conditions. The inferior aspect of the temporal lobe is typically involved in thanatophoric dysplasia, whereas the medial aspects of the temporal and occipital lobes are more characteristic locations in achondroplasia [19].

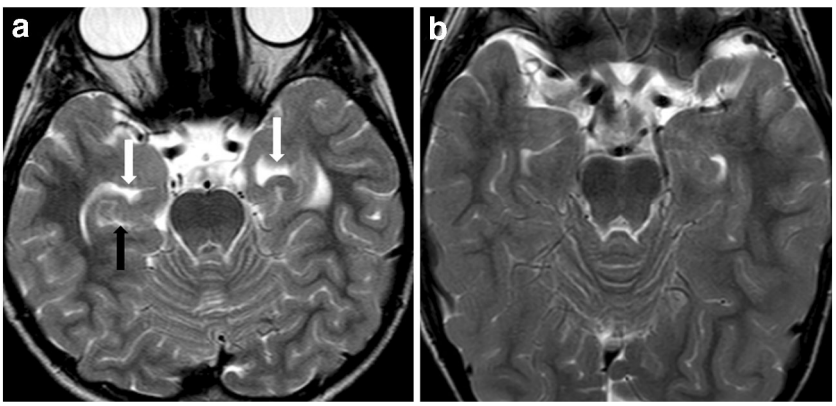

Fig. 16 Abnormal triangular shape of the temporal horn in an 11-year-old girl with achondroplasia. **a** Axial T2-weighted MR image (repetition time/echo time [TR/TE]: 5,500/100 ms) shows triangular shape of the temporal horns of the lateral ventricles (*white arrows*). Note the deep transverse sulcus (*black arrow*). **b** Axial T2-weighted MR image (TR/TE: 5,500/100 ms) of a normal child for comparison shows the normal morphology of the temporal horns of the lateral ventricles

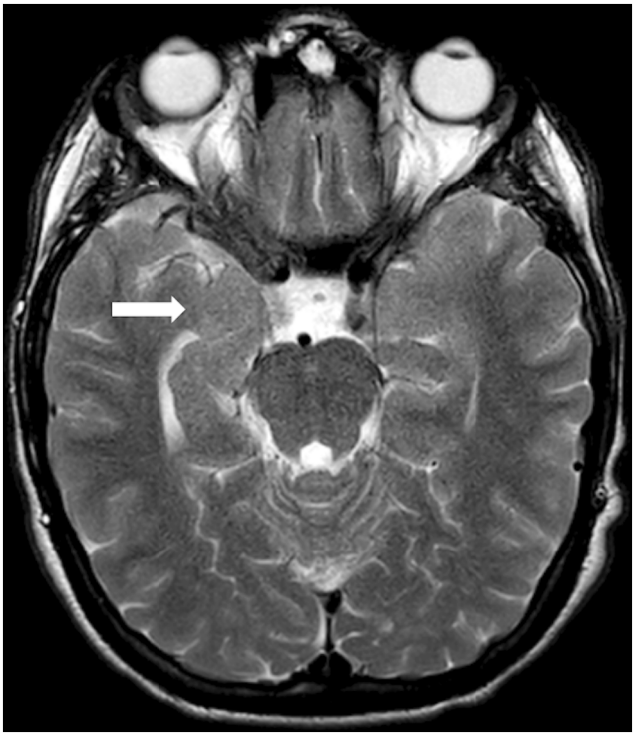

Fig. 17 Loss of gray–white matter differentiation in a 9-year-old boy with achondroplasia. Axial T2-weighted MR image (repetition time/echo time: 5,500/100 ms) demonstrates a loss of gray–white matter differentiation of the mesial temporal lobe (*arrow*). The finding is subtle

- **Abnormal triangular shape of the temporal horn of lateral ventricle:** Abnormal triangular shape was observed in 46% of the children with achondroplasia [6]. The triangular shape of part of the lateral ventricular might be related to dysplastic changes and the transverse sulcus of the mesial temporal lobe (Fig. 16). The triangular morphology of the temporal horn can be observed on axial images.
- **Loss of gray–white matter differentiation:** Loss of the gray–white matter differentiation has been demonstrated in achondroplasia [6]. Cortical thickening and loss of the gray–white matter differentiation can be observed on axial and coronal MR images (Fig. 17).
- **Megalencephaly and temporal lobe enlargement:** Megalencephaly is defined as excessive cerebral growth [24]. Ventriculomegaly generally accompanies this finding. Although megalencephaly is reported to be a relatively less common condition with a frequency of 38% [6], it might be an early neurologic finding of achondroplasia and cause cognitive deficits in some children [25]. Assessing this finding is sometimes problematic because the other brain findings in achondroplasia including macrocephaly, frontal and parietal bossing, and enlarged subarachnoid spaces can cause the brain to seem relatively small. The temporal lobe enlargement is defined as an overgrowth of the surface of the temporal lobe beyond the border of the adjacent frontal and parietal lobes on coronal images [6] (Fig. 18).

Craniocervical junction

Narrowing of the foramen magnum

Narrowing of the foramen magnum is a characteristic finding of achondroplasia. An abnormal placement and premature fusion of the posterior synchondroses also lead to foramen magnum stenosis as well as the endochondral ossification defects [10]. In a recent study by Bosemani et al. [8], the foramen magnum surface area was approximately 6 times and the jugular foramen surface area 10 times smaller in children with achondroplasia when compared to age-matched controls. The findings can cause hydrocephalus and prominent emissary and meningeal veins. Besides this, one of the most severe consequences of the foramen magnum narrowing is cervicomedullary compression [10]. It is

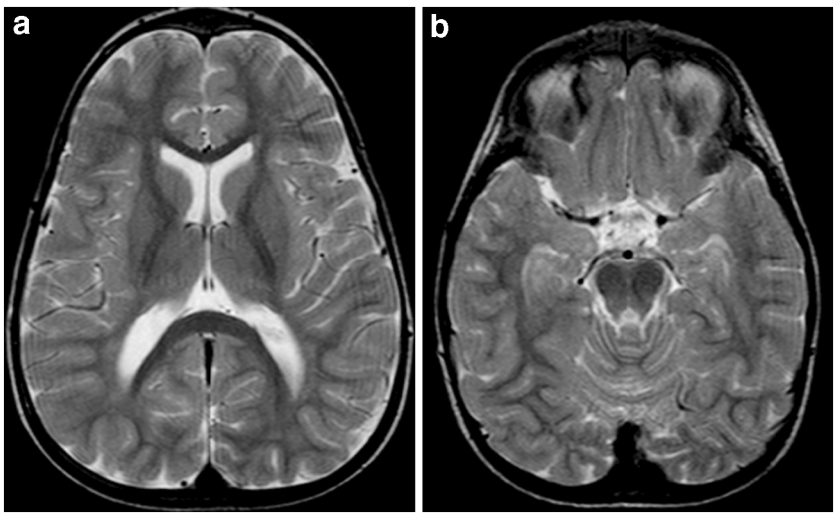

Fig. 18 Megalencephaly and temporal lobe enlargement in a 2-year-old boy with achondroplasia. **a, b** Axial T2-weighted MR images (TR/TE: 5,500/100 ms) at the level of the basal ganglia (**a**) and mesencephalon (**b**) show an increased brain volume. The finding is more noticeable within the temporal lobes

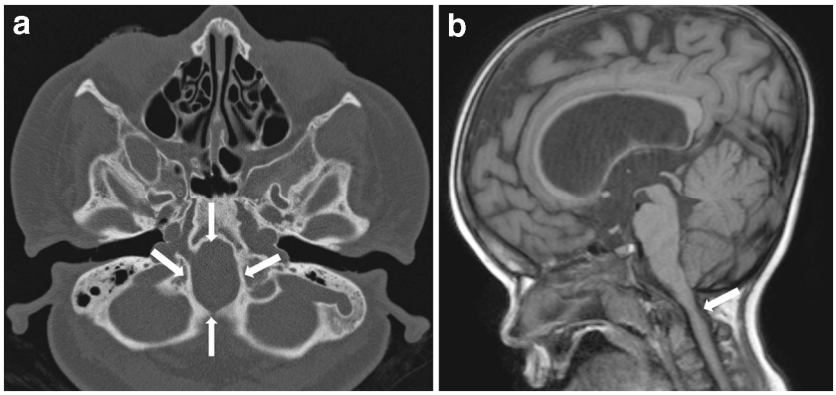

Fig. 19 Narrowing of the foramen magnum in a 4-year-old boy with achondroplasia. **a** Axial CT image shows the narrowing of the foramen magnum (*arrows*). **b** Sagittal T1-weighted MR image (repetition time/echo time: 500/15 ms) demonstrates the narrowing of the foramen magnum, and the compression of the medulla and upper cervical spinal cord in this child (*arrow*). Ventricular dilatation is also seen

associated with severe morbidity and even sudden death, especially in children 4 years or younger [10]. Both CT and MR images can be used to measure foramen magnum dimensions (Fig. 19). While performing imaging, the head and neck position is sometimes not suitable for optimal assessment of the foramen magnum because of the increased head size and accompanying neurologic deficits. Reformatted images obtained parallel to the plane between the basion and opisthion provide more accurate measurements.

Myelopathy

Myelopathy of the upper cervical spinal cord is a frequent finding in achondroplasia. The clinical symptoms of the upper cervical spinal cord injury have a wide spectrum range from neck pain to neurologic disability, and respiratory and cardiopulmonary complications [26]. Although the narrowing of the foramen magnum is a characteristic finding of achondroplasia, there has been no consensus whether this narrowing is the main cause of cervical myelopathy in childhood [27–29]. The atlanto-axial instability that is usually associated with os odontoideum has also been reported as a responsible factor for cervical spinal cord injury symptoms [30]. Radiography of the cervical spine (flexion and extension), CT scanning and MR imaging can be used as diagnostic tools in cases of suspicion for atlanto-axial instability. Os odontoideum can be recognized easily on CT scan and plain radiographs. It is seen as an ossicle with rounded, cortical borders that is separated by a variable gap from the odontoid process. MR imaging demonstrates the myelopathic signal changes in the cervical spine rather than bone abnormalities. Dynamic MR imaging studies provide valuable information about the postural-induced atlanto-axial instability. In addition to the radiologic tools, polysomnography is also recommended because most children with achondroplasia also have apnea [31]. Myelomalacia is seen as high-signal intensity on T2-weighted images (Fig. 20). Intramedullary cystic changes, which indicate the cystic myelomalacia, can also be seen, especially in untreated children. High-signal-intensity lesions in the cervical spinal cord have also been described without the accompanying compression or atlanto-axial instability in children with achondroplasia [7]. In a study of postmortem neuropathological changes in cases of confirmed achondroplasia, histological changes in the cervical spinal cord were found similar to those of traumatic central cord syndrome [26]. They supposed that these changes might occur because of arterial insufficiency rather than direct impact. Radiologists should note that the pathological signal changes in the spinal

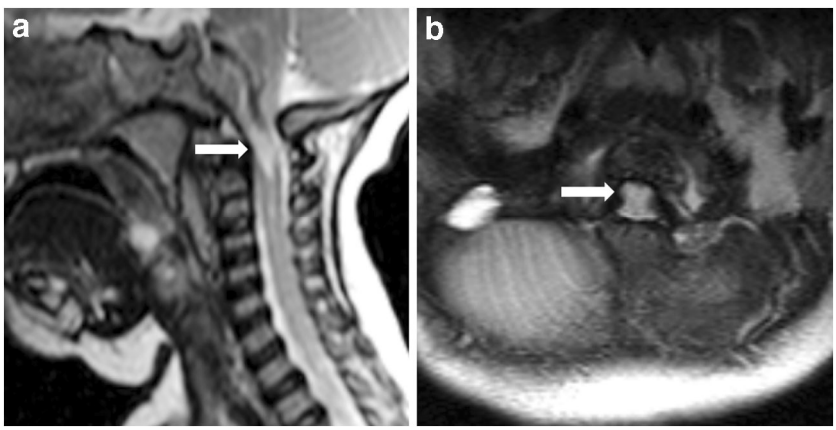

Fig. 20 Myelopathy in a 6-year-old girl with achondroplasia. **a, b** Sagittal (**a**) and axial (**b**) T2-weighted MR images (repetition time/echo time: 5,500/100 ms) show the high signal intensity within the medulla and upper cervical spinal cord (*arrows*). The finding is compatible with myelomalacia

cord can occur even if significant clinical symptoms, narrowing of the foramen magnum, and signs for atlanto-axial instability are not present [5].

Conclusion

The neuroimaging and craniofacial findings described here are not uncommon in achondroplasia. Radiologists should be aware of these findings because they have an important role in the diagnosis of achondroplasia and the recognition of complications.

Compliance with ethical standards

Conflicts of interest None

References

1. Shiang R, Thompson IM, Zhu YZ et al (1994) Mutations in the transmembrane domain of FGFR3 cause the most common genetic form of dwarfism, achondroplasia. Cell 78:335–342
2. Pauli RM (2019) Achondroplasia: a comprehensive clinical review. Orphanet J Rare Dis 14:1
3. Al-Saleem A, Al-Jobair A (2010) Achondroplasia: craniofacial manifestations and considerations in dental management. Saudi Dent J 22:195–199
4. Collins WO, Choi SS (2007) Otolaryngologic manifestations of achondroplasia. Arch Otolaryngol Head Neck Surg 133:237–244
5. Brühl K, Stoeter P, Wietek B et al (2001) Cerebral spinal fluid flow, venous drainage and spinal cord compression in achondroplastic children: impact of magnetic resonance findings for decompressive surgery at the cranio-cervical junction. Eur J Pediatr 160:10–20
6. Manikkam SA, Chercuti K, Howell KB et al (2018) Temporal lobe malformations in achondroplasia: expanding the brain imaging phenotype associated with FGFR3-related skeletal dysplasias. AJNR Am J Neuroradiol 39:380–384
7. Brouwer PA, Lubout CM, van Dijk JM, Vleggeert-Lankamp CL (2012) Cervical high-intensity intramedullary lesions in achondroplasia: aetiology, prevalence and clinical relevance. Eur Radiol 22: 2264–2272
8. Bosemani T, Orman G, Hergan B et al (2015) Achondroplasia in children: correlation of ventriculomegaly, size of foramen magnum and jugular foramina, and emissary vein enlargement. Childs Nerv Syst 31:129–133
9. Kao SC, Waziri MH, Smith WL et al (1989) MR imaging of the craniovertebral junction, cranium, and brain in children with achondroplasia. AJR Am J Roentgenol 153:565–569
10. Bagley CA, Pindrik JA, Bookland MJ et al (2006) Cervicomedullary decompression for foramen magnum stenosis in achondroplasia. J Neurosurg 104:166–172
11. Cobb SR, Shohat M, Mehringer CM, Lachman R (1988) CT of the temporal bone in achondroplasia. AJNR Am J Neuroradiol 9:1195–1199
12. Jin SW, Sim KB, Kim SD (2016) Development and growth of the normal cranial vault: an embryologic review. J Korean Neurosurg Soc 59:192–196
13. Jung J, Yang C, Lee S, Choi J (2013) Bilateral ossiculoplasty in 1 case of achondroplasia. Korean J Audiol 17:142–147
14. Steinbok P, Hall J, Flodmark O (1989) Hydrocephalus in achondroplasia: the possible role of intracranial venous hypertension. J Neurosurg 71:42–48
15. Sainte-Rose C, LaCombe J, Pierre-Kahn A et al (1984) Intracranial venous sinus hypertension: cause or consequence of hydrocephalus in infants? J Neurosurg 60:727–736
16. DiMario FJ Jr, Ramsby GR, Burleson JA, Greensheilds IR (1995) Brain morphometric analysis in achondroplasia. Neurology 45: 519–524
17. Wolpert SM (1969) Dural sinus configuration: measure of congenital disease. Radiology 92:1511–1516
18. Moritani T, Aihara T, Oguma E et al (2006) Magnetic resonance venography of achondroplasia: correlation of venous narrowing at the jugular foramen with hydrocephalus. Clin Imaging 30:195–200
19. Pugash D, Lehman AM, Langlois S (2014) Prenatal ultrasound and MRI findings of temporal and occipital lobe dysplasia in a twin with achondroplasia. Ultrasound Obstet Gynecol 44:365–368
20. Philpott CM, Widjaja E, Raybaud C et al (2013) Temporal and occipital lobe features in children with hypochondroplasia/FGFR3 gene mutation. Pediatr Radiol 43:1190–1195
21. Lu L, Airey DC, Williams RW (2001) Complex trait analysis of the hippocampus: mapping and biometric analysis of two novel gene loci with specific effects on hippocampal structure in mice. J Neurosci 15:3503–3514
22. Cury C, Toro R, Cohen F et al (2015) Incomplete hippocampal inversion: a comprehensive MRI study of over 2,000 subjects. Front Neuroanat 9:160
23. Rossi MA (2017) The malrotated hippocampal formation: how often must we judge function by shape? Epilepsy Curr 17:88–90
24. Pavone P, Praticò AD, Rizzo R et al (2017) A clinical review on megalencephaly: a large brain as a possible sign of cerebral impairment. Medicine 96:e6814
25. Dennis JP, Rosenberg HS, Alvord EC Jr (1961) Megalencephaly, internal hydrocephalus and other neurological aspects of achondroplasia. Brain 84:427–445
26. Yang SS, Corbett DP, Brough AJ et al (1977) Upper cervical myelopathy in achondroplasia. Am J Clin Pathol 68:68–72
27. Keiper GL Jr, Koch B, Crone KR (1999) Achondroplasia and cervicomedullary compression: prospective evaluation and surgical treatment. Pediatr Neurosurg 31:78–83
28. Reid CS, Pyeritz RE, Kopits SE et al (1987) Cervicomedullary compression in young patients with achondroplasia: value of comprehensive neurologic and respiratory evaluation. J Pediatrics 110: 522–530
29. Morgan DF, Young RF (1980) Spinal neurological complications of achondroplasia. Results of surgical treatment J Neurosurg 52: 463–472
30. Mohindra S, Tripathi M, Arora S (2011) Atlanto-axial instability in achondroplastic dwarfs: a report of two cases and literature review. Pediatr Neurosurg 47:284–287
31. Waters KA, Everett F, Sillence D et al (1993) Breathing abnormalities in sleep in achondroplasia. Arch Dis Child 69:191–196